INTERNATIONAL SOCIETY FOR SOIL MECHANICS AND GEOTECHNICAL ENGINEERING



This paper was downloaded from the Online Library of the International Society for Soil Mechanics and Geotechnical Engineering (ISSMGE). The library is available here:

https://www.issmge.org/publications/online-library

This is an open-access database that archives thousands of papers published under the Auspices of the ISSMGE and maintained by the Innovation and Development Committee of ISSMGE.

The paper was published in the proceedings of the 20th International Conference on Soil Mechanics and Geotechnical Engineering and was edited by Mizanur Rahman and Mark Jaksa. The conference was held from May 1st to May 5th 2022 in Sydney, Australia.

Microscopic mechanism on permeability anisotropy of Hangzhou clay

Mécanisme microscopique sur l'anisotropie de perméabilité de l'argile de Hangzhou

Jian Zhou, Hao Hu & Xiao Zhang

Research Center of Coastal and Urban Geotechnical Engineering, Zhejiang University, China, zjelim@zju.edu.cn

Ling-hui Luo

Shanghai Municipal Engineering Design Institute (Group) CO.,LTD.,China

ABSTRACT: A research on the permeability anisotropy of undisturbed soil has important guiding significance for engineering applications. In this paper, a series of experiments were conducted by triaxial permeameter to find out the permeability anisotropy of Hangzhou undisturbed clay, thereby establishing the permeability anisotropy model. The results show that the hydraulic conductivity of Hangzhou clay decreases with the increase of consolidation pressure, the permeability anisotropy r_k increases with the increase of consolidation pressure increases, the number of pores increases and the pore area decreases. The horizontal pore area of Hangzhou clay is higher than the vertical one however, the pore area cannot accurately reflect the permeability anisotropy since some overhead structures are closed and will not participate in seepage. Hence, it is more reasonable to study the permeability anisotropy of undisturbed clay from the perspective of continuity of pore distribution. Finally, a permeability anisotropy model of Hangzhou undisturbed clay is obtained by micro parameter pore index D_{50} .

RÉSUMÉ : Une recherche sur l'anisotropie de perméabilité d'un sol non perturbé a une importance décisive pour les applications d'ingénierie. Dans cet article, une série d'expériences ont été menées par perméamètre triaxial pour découvrir l'anisotropie de perméabilité de l'argile non perturbée de Hangzhou, établissant ainsi le modèle d'anisotropie de perméabilité. Les résultats montrent que la conductivité hydraulique de l'argile de Hangzhou diminue avec l'augmentation de la pression de consolidation, l'anisotropie de perméabilité r_k augmente avec l'augmentation de la pression de consolidation augmente, le nombre de pores augmente et la surface des pores diminue. La surface des pores horizontaux de L'argile de Hangzhou est plus haute que l'argile verticale cependant, la surface des pores ne peut pas refléter avec précision l'anisotropie de perméabilité puisque certaines structures aériennes sont fermées et ne participeront pas à l'infiltration. Par conséquent, il est plus raisonnable d'étudier l'anisotropie de perméabilité de l'argile non perturbée du point de vue de continuité des pores di Enfin, un modèle d'anisotropie de perméabilité de l'argile non perturbée de Hangzhou est obtenu par l'indice de pore de micro-paramètre D_{50} .

KEYWORDS: Hydraulic conductivity, permeability anisotropy, undisturbed clay, microscopic analysis, pore index

1 INTRODUCTION.

The permeability of clay soil has a great impact on tunneling or other underground/underwater construction. However it is mainly considered as isotropic, which cannot reflect the real anisotropic property and may cause unsafe design. Therefore, it is necessary to study the permeability anisotropy of undisturbed clay systematically.

Clay soil has a certain permeability anisotropy under long-term sedimentation. A large number of studies have shown that the hydraulic conductivity of soil in the direction of deposition is significantly higher than that in other directions, that is, the hydraulic conductivity parallel to the deposition plane is greater than that perpendicular to the deposition plane (Yu Liang-gui 2019, Leroueil et al. 1990, Basak 1972, Kenney & Chan 1973). The ratio of the horizontal hydraulic conductivity k_n and vertical hydraulic conductivity k_v is defined as the permeability anisotropy r_k , and it is often used to represent the permeability anisotropy of soil (Leroueil et al. 1990, Tavenas et al. 1983, Adams et al. 2016).

In the experiments by Leroueil et al. (1990), the r_k of Louiseville soil was found to be 1.35~1.55 when the strain of the soil was less than 25%. The test results from Adams et al. (2013) showed that the r_k of Boston red clay gradually increased from 1.2 to 1.9 with the gradual decrease of soil void ratio. Chapuis et al. (1989) found that the permeability anisotropy of sand and clay is an exponential relationship with the void ratio, the smaller the void ratio was, the greater the permeability anisotropy was, and

obtained a permeability anisotropy model expressed by void ratio. Adams et al. (2013) also established the permeability anisotropy model in terms of void ratio based on the experiment data of Boston blue clay.

Most of the researches on permeability anisotropy are based on macro level. Witt et al. (1983) pointed out that there are three reasons leading to the permeability anisotropy of soft clay, which are macroscopic stratification, microscopic stratification and particle trend. The microscopic pore distribution characteristics of soil has great influence on the hydraulic conductivity. Water infiltration in the soil is essentially working as the water flow in the pore, but the pore distribution is irregular and nonlinear. The microstructure of soil with the same void ratio behaves differently. Adams et al. (2016) also found that the permeability anisotropy of soil is mainly affected by soil porosity and particle orientation arrangement. Thus, the model only considers macro parameters such as void ratio and strain cannot reveal the essence of the permeability anisotropy.

In this paper, studies were performed on Hangzhou undisturbed clay. Triaxial permeability samples are cut from the horizontal and vertical directions to determine the hydraulic conductivity and to calculate the permeability anisotropy. The microstructure of the samples after seepage is systematically studied to explore the influence on permeability anisotropy, based on which a micro permeability anisotropy model of Hangzhou undisturbed clay is proposed. This research provides a new perspective from micro level and will be references for permeability study on fine particle materials.

2 MATERIALS AND METHODS

2.1 Test sample

The test samples were collected from a 5m depth foundation pit in Hangzhou. The basic physical and mechanical properties are shown in Table 1. The soil sample was first cut into $100 \text{mm} \times 50 \text{mm}$ (height \times diameter) along the horizontal and vertical directions under the sample cutter. Then the cylindrical samples were installed on the GDS triaxial permeameter for seepage experiments to measure the k_h and k_v of the clay.

Table 1. Basic physical and mechanical properties of soil

Parameter	
Weight γ $(kN \cdot m^{-3})$	17.1
Void ratio <i>e</i>	1.25
Water content ω (%)	43.2
Specific gravity G_S	2.68
Liquid limit ω_L (%)	48.7
Plastic limit ω_P (%)	22.6

2.2 Penetration test

In order to explore the in-situ permeability anisotropy in the greatest extend in the laboratory, undisturbed clay was used for the permeability test research. Considering the characteristics of undisturbed soil heterogeneity, three repeated tests were conducted for under each test condition, and the average data of three tests were taken as the representative one. The test scheme was presented as shown in Table 2.

Table 2. Experiment Schemes

Test Number	Infiltration direction	Consolidation pressure (kPa)	
VP1	vertical	100	
HP1	horizontal	100	
VP2	vertical	200	
HP2	horizontal	200	
VP3	vertical	300	
HP3	horizontal	300	

Put the cut sample in the vacuum saturation cylinder to pump air for saturation for 24h, then install the pre saturated sample on the GDS triaxial permeameter, and the test steps of saturation, consolidation and seepage are carried out to complete the whole seepage experiment. The specific content and operation of each loading step are as follows:

- (1) Saturation stage: saturate the sample at a back pressure of 100kPa, and ensure the Skempton's pore pressure parameter B was greater than 0.98.
- (2) Consolidation stage: consolidate the sample under the preset effective pressure, until the drainage volume was less than 100 mm³ per 3600 s.
- (3) Seepage stage: according to the standard (ASTM, 2010), the reference pressure was designed as $100+\Delta u/2$ (kPa), and the back pressure was designed as $100-\Delta u/2$ (kPa), where Δu was the pressure difference between the bottom and top of the soil under

the design hydraulic gradient. In this test, the hydraulic gradient was set to 40 according to Yu's study (2019) on hydraulic gradient.

2.3 Microscopic test methods

2.3.1 Microscopic observation methods of temples

The sample after the seepage test was cut into a 20 mm \times 5 mm \times 5 mm (height \times length \times width) sample along the seepage direction as the sample for the micro test. Then the SEM images of Hangzhou undisturbed clay were obtained by electron microscope scanning technology.

Undisturbed clay has many macro pores and overhead structures (Zhou, 2014) which have a great impact on the permeability characteristics. Therefore, the SEM photographs adopted in this paper were all taken at 1200 times magnification to photograph the complete macro porous structure.

2.3.2 Quantitative analysis methods of SEM images

The size of the SEM photographs were 1024×885 pixels. The actual size of images was $246.78 \times 213.29 \mu m$ after the scale transformation, that is, each pixel corresponds to $0.24129 \mu m$. For convenience, the microscopic parameters related to pore area are calculated by pixel in this paper. At the same time, in order to overcome the contingency caused by uneven pore distribution of undisturbed soil, three observation points were randomly selected for microscopic shooting of the observed samples under each study state and the average value of pore area data obtained from the three observation points was taken for subsequent quantitative analysis.

The quantitative processing of pore area of SEM images is carried out by using the Particles and Cracks Analysis System (PCAS) developed by Liu Chun et al. (2011) of Nanjing University. The main process consists of two steps: (1) Binarization of SEM images to identify pores and particles; (2) The binarization image which is further vectored and after the image is processed, the relevant parameters such as pore area quantitatively analyzed.

3 TEST RESULTS

3.1 Penetration test results

Table 3 presents the results of permeability test of Hangzhou undisturbed clay under various consolidation pressures. The variation of hydraulic conductivity and permeability anisotropy of samples under different consolidation pressures is shown in Figure 1.

Table 3. Penetration test results

Test Number	k_h	k_v	r_k	e
P1	1.070	0.956	1.12	0.982
P2	0.652	0.533	1.222	0.892
Р3	0.356	0.282	1.263	0.835

With the increase of consolidation pressure, the hydraulic conductivity decreases linearly, but the slope of the permeability curve is slightly higher when the consolidation pressure changes from 100kPa to 200kPa, which is slightly higher than that when the consolidation pressure changes from 200kPa to 300kPa, which shows that the compactness of test sample increases with the increase of consolidation pressure. The increases with the increase of consolidation pressure. It increases rapidly under low stress condition, and increases slowly under high stress condition.

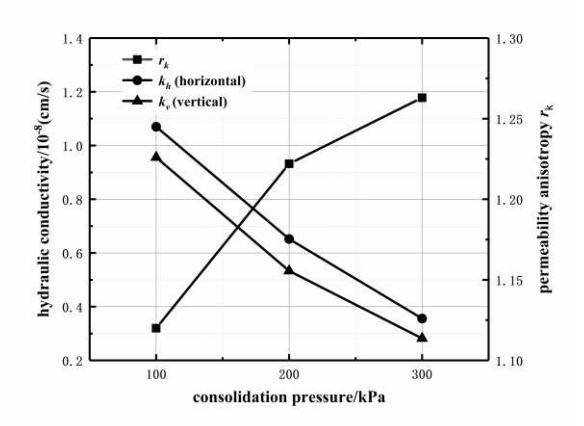


Figure 1. Changes of hydraulic conductivity and permeability anisotropy r_k under different consolidation pressures.

The variation of permeability anisotropy under different consolidation pressure is consistent with the experimental law of Clennell et al. (1999), Adams et al. (2016), Luo Ling-hui (2020).

According to the test in this paper, the permeability anisotropy r_k of undisturbed clay in Hangzhou is about 1.12-1.26. Table 4 shows the permeability anisotropy of several clays. It can be seen that the r_k of most undisturbed clay is 1.1-1.6. The engineering properties of Xiaoshan clay and Shanghai clay are similar to those of Hangzhou clay, and the permeability anisotropy are also close.

Table 4. Microscopic test results

Types of soil	Consolidation pressure or void ratio range	r_k	Reference
Hangzhou undisturbed clay in this paper	$100\text{kPa} \leq p \leq 300\text{kPa}$	1.12-1.26	this paper
Undisturbed Xiaoshan clay	$50kPa \leq p \leq 400kPa$	1.32-1.34	Dong Yi-ning (2020)
Louiseville soil	$1 \leq e \leq 1.95$	1.35-1.55	Leroueil (1990)
Bäckebol soil	$1.4 \leq e \leq 2.2$	1.18-1.33	Leroueil (1990)
Undisturbed Shanghai clay	$12.5kPa \leq p \leq 400kPa$	1.2-1.6	Song Yun-qi (2018)
Boston red clay	$0.4\text{MPa} \leq p \leq 10\text{MPa}$	1.2-1.9	Adams (2016)

3.2 Qualitative analysis of SEM photos

Figure 2 shows the microscopic images of clay under different consolidation pressures and seepage directions. The soil particles observed in the vertical direction are flake or plate-shaped; the soil particles observed in the horizontal direction are honeycomb and granular with the distribution of particles and pores more disorderly. At the same time, the number of pores in the horizontal direction is more than that in the vertical direction. Under the lower consolidation pressure (100kPa), the soil has larger pores and fissures which are the microcosmic essence of higher hydraulic conductivity of soil under lower consolidation pressure. With the increase of consolidation pressure, the large pores decrease, the small pores increase, the plate-shaped aggregates of vertical soil particles become denser, the horizontal pore area decreases, the number of pores increases and the honeycomb shape becomes more significant.

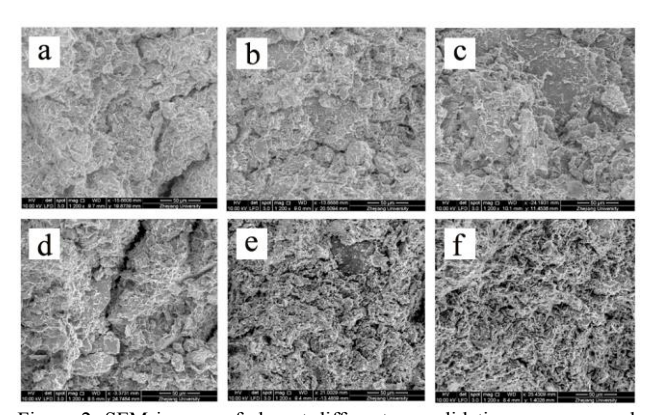


Figure 2. SEM images of clay at different consolidation pressures and infiltration directions (1200 times magnification): a) P1 vertical view (100kPa), b) P2 vertical view (200kPa), c) P3 vertical view (300kPa), d) P1 horizontal view (100kPa), e) P2 horizontal view (200kPa), f) P3 horizontal view (300kPa).

3.3 Quantitative analysis of pore area

The pore size inside the soil is an important factor affecting the permeability characteristics. Figure 3 shows the variation trend of the pore area, pore area ratio γ_s and permeability anisotropy r_k in different directions of undisturbed clay in Hangzhou under different consolidation pressures, in which

$$\gamma_s = S_h / S_v \tag{1}$$

Where S_h , S_v is the pore area of horizontal and vertical seepage profiles respectively.

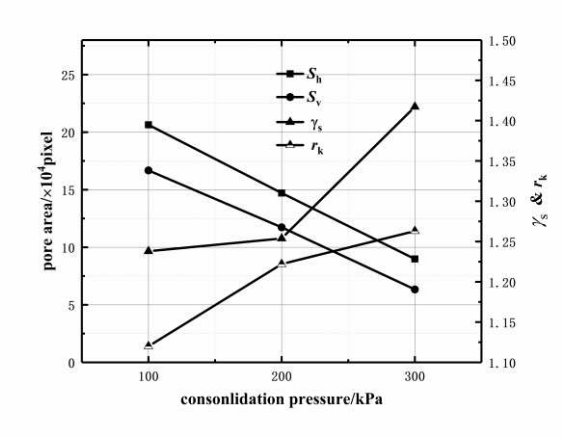


Figure 3. Changes of pore area, pore area ratio γ_s and permeability anisotropy r_k with consolidation pressure.

Both horizontal and vertical pore areas decrease continuously with the increase of consolidation pressure. This is consistent with the conclusion that the hydraulic conductivity decreases with the increase of consolidation pressure and also explains the essential reason of the change of hydraulic conductivity from the

microscopic. The pore area ratio γ_s and permeability anisotropy r_k increase with the increase of consolidation pressure. However, when the consolidation pressure is greater than 200 kPa, the increase rate of pore area ratio r_k is accelerated while the increase rate of permeability anisotropy r_k slowed down. This manifests that the change law of pore area ratio γ_s cannot fully reflect the change law of permeability anisotropy r_k .

Although pore area can indirectly reflect the change of pore volume in three-dimensional space, it cannot however well reflect the change of permeability anisotropy. Cui De-shan et al. (2010) found that the thickness of the weakly bound water membrane of the clay soil was about 0.12 μm, while Dang Faning et al. (2015) considered that the pores occupied by this part of the weakly bound water were invalid pores that did not participate in seepage. As shown in Figure 4, only when the pore size is greater than 2 times the thickness of weakly bound water membrane, can water flow through the pores under the action of permeability. Wang Xiu-yan (2013) investigated that only under high stress, weak bound water will participate in the seepage. At the same time, undisturbed soil has some overhead structures (Huang Li 2007) and part of them are closed which do not participate in seepage. Thus, it can be concluded that an accurate permeability anisotropy model cannot be obtained only from the perspective of pore area.

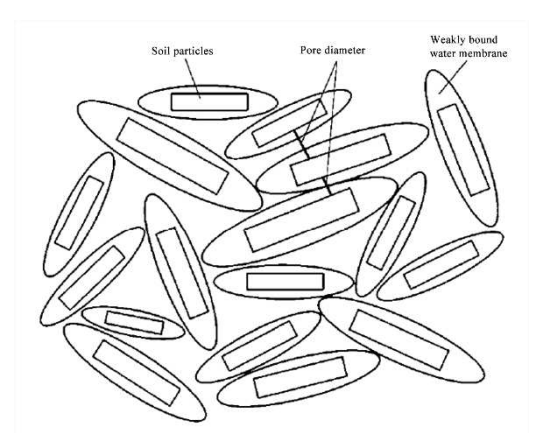


Figure 4. Adsorbed water layers of clay particles (Zhou Jian 2019)

4 DISCUSSION OF MICROSCOPIC MODEL

4.1 Definition of microscopic parameters

Tanaka et al. (2003) measured the hydraulic conductivity of different clay and obtained the corresponding pore gradation curve of corresponding clay through Mercury Intrusion Porosimetry (MIP). It was found that there was a good linear relationship between the hydraulic conductivity and the pore size coefficient r_{50}^2 (where r_{50} is the pore diameter corresponding to the pore area less than 50% of the total pore area on the pore

gradation curve). Xu Jie et al. (2020) measured the hydraulic conductivity and permeability anisotropy of kaolin-montmorillonite mixed clay, it was found that there was a good linear relationship between the permeability anisotropy and the pore index D_{70} , in which

$$D_{70} = r_{h70}^2 / r_{v70}^2 (2)$$

Where r_{h70} , r_{v70} is the pore size corresponding to 70% of the total pore area on the pore gradation curve of horizontal and vertical seepage profiles.

Now the pore indexes of different consolidation pressures and different seepage profiles are selected as the research object. The definition of the pore index D_{20} , D_{30} , D_{40} , D_{50} , D_{60} was obtained by analogy with Eq.2.

4.2 Microscopic model study

Most of the infiltration models adopt the semi-logarithmic relationship, so this paper still takes the semi-logarithmic relationship as the basis to explore the relationship between the permeability anisotropy and the microscopic parameters (D_{20} , D_{30} , D_{40} , D_{50} , D_{60}). The macro and micro parameters obtained by the experiment in this paper are shown in Table 5, and the permeability anisotropy in Table 5 is fitted with each micro parameter respectively. The obtained correlation coefficient is summarized in Table 6 in order to compare the correlation of each fitting result more intuitively.

For the fitting of pore index, the correlation between pore index D_{20} , D_{30} , D_{40} and permeability anisotropy is not satisfactory. In the experiment of remolded soil, the larger the pore index is, the larger the pore area will be, and the better it can reflect the permeability characteristics of soil (Xu Jie 2020). However, when the pore index of undisturbed soil increased to D_{50} , the correlation coefficient of fitting begins to decrease. This difference is due to the existence of overhead structure in undisturbed soil (Zhou Jian 2014, Huang Li 2007, Ri-qing Xu 2016) which has a great impact on the pore area in the direction of permeability. Since some of the overhead structures are closed pores and do not participate in seepage, which makes it impossible to accurately reflect the change of permeability anisotropy when the pore index is large.

The permeability anisotropy model obtained by fitting has a high correlation coefficient when the pore index is $D_{40} \sim D_{60}$, among which the correlation coefficient of the model fitted by pore index D_{50} is the highest, which is 0.966. So, a permeability anisotropy model of Hangzhou undisturbed clay is obtained by fitting pore index D_{50} , which is

$$lg_{rk} = 0.191D_{50} - 0.174$$
 (3)

Table 5	Microso	copic test	results
Table 5.	MICIOS	LODIC ICSI	icsuits

Consolidation pressure(kPa)	lg_{rk}	γ_s	D_{20}	D ₃₀	D_{40}	D_{50}	D ₆₀	D ₇₀
100	0.049	1.238	1.146	1.280	1.248	1.179	1.283	1.425
200	0.087	1.254	1.153	1.216	1.353	1.335	1.328	1.513
300	0.101	1.417	1.265	1.419	1.459	1.455	1.371	1.272

Table 6. Microscopic permeability anisotropy model

Number	Parameter (x)	lg_{rk} (y)	The correlation coefficient R^2
1	γ_s	y=0.207x-0.191	0.582
2	D_{20}	y=0.300x-0.277	0.554
3	D_{30}	y=0.118x-0.075	0.208
4	D_{40}	y=0.246x-0.254	0.932
5	D_{50}	y=0.191x-0.174	0.966
6	D_{60}	y=0.593x-0.708	0.940
7	D_{70}	y=-0.090x+0.205	0.165

5 CONCLUSIONS

In this paper, the permeability anisotropy of Hangzhou undisturbed clay is studied by means of seepage test and micro analysis.

- (1) The hydraulic conductivity of Hangzhou undisturbed clay decreases with the increase of consolidation pressure; the permeability anisotropy increases with the increase of consolidation pressure, and the increase range of anisotropy ratio decreases with the increase of consolidation pressure; the permeability anisotropy of Hangzhou undisturbed clay is about 1.12-1.26.
- (2) There are large differences in SEM photos of Hangzhou undisturbed clay in different infiltration directions. The soil particles observed in the vertical direction are sheet or plate-shaped; the soil particles observed in the horizontal direction are honeycomb and granular and the distribution of particles and pores is more chaotic. With the increase of consolidation pressure, the number of pores increases and the area of pores decreases. The plate-like aggregates of vertical soil particles are much denser, and the honeycomb structure of horizontal soil particles is more significant.
- (3) The pore area of Hangzhou undisturbed clay in horizontal direction is higher than that in vertical direction but the permeability anisotropy cannot be accurately manifested only from the pore area. It is more reasonable to study the permeability anisotropy of undisturbed clay from the perspective of continuity of pore distribution. A permeability anisotropy model of Hangzhou undisturbed clay is obtained by fitting pore index D_{50} .

6 ACKNOWLEDGEMENTS

This study was supported by the National Natural Science Foundation of China (Grant numbers 52078455, 51708507) and National Key Research and Development plan of China (Grant Number 2016YFC0800203).

7 REFERENCES

- Adams A L, Germaine J T, Flemings P B, et al. 2013. Stress induced permeability anisotropy of Resedimented Boston Blue Clay. Water Resources Research 49(10):6561-6571.
- Adams A L, Nordquist T J, Germaine J T, et al. 2016. Permeability anisotropy and resistivity anisotropy of mechanically compressed mudrocks. *Canadian Geotechnical Journal*. (9), doi:.
- Astm D. 2010. Standard test methods for measurement of hydraulic conductivity of saturated porous materials using a flexible wall permeameter. Astm International West Conshohocken: 1-24.
- Basak P. 1972. Soil Structure and its effects on hydraulic conductivity . Soil Science 114(6): 417-422.

- Chapuis R P, Gill D E. 1989. Hydraulic anisotropy of homogeneous soils and rocks: influence of the densification process. *Bulletin of Engineering Geology & the Environment* 39(1):75-86.
- Cui De-shan, Xiang Wei, Cao Li-jing, et al. 2010. Experimental study on reducing thickness of adsorbed water layer for red clay particles treated by ionic soil stabilizer. *Chinese Journal of Geotechnical Engineering* 32(6):944–949. (in Chinese)
- Dang Fa-ning, Liu Hai-wei, Wang Xue-wu et al. 2015. Empirical formulas of permeability of clay based on effective void ratio. *Chinese Journal of Rock Mechanics and Engineering* 34(09): 1909-1917(in Chinese)
- Dong Yi-ning, Xu Ri-qing, Gong Xiao-nan. 2020. Experimental study on the influence of the structure of Xiaoshan clay on permeability. *Dam Observation and Geotechnical Tests* 24(6): 44-46
- Huang Li. 2007. Quantitative analysis of micro-porosity of saturated soft clay and its fractal description. Wuhan University of Technology.
- Kenney T C, Chan H T. 1973. Field investigation of permeability ratio of New Liskeard Varved Soil. *Canadian Geotechnical Journal* 10(3):473-488.
- Leroueil S, Bouclin G, Tavenas F, et al. 1990. Permeability anisotropy of natural clays as a function of strain. *Canadian Geotechnical Journal* 27(5):568-579.
- Liu C, Shi B, Zhou J, et al. 2011. Quantification and characterization of microporosity by image processing, geometric measurement and statistical methods: Application on SEM images of clay materials. *Applied Clay Science* 54(1):97-106.
- Luo Ling-hui. 2020. Experimental study and application about static and dynamic seepage test of soft clay based on HCA[D]. Hangzhou: Zhejiang University.
- M. B. Clennell, D. N. Dewhurst, K. M. Brown et al. 1999. Permeability anisotropy of consolidated clays. *Geological Society*, London, Special Publications (158),79-96.
- Ri-qing Xu, Li-yang Xu, Jin-chuan Duan, Xin Xu, Jiang-shan Fu and Xiao-bin Wu. 2016. Microstructure morphology and optimization of influencing factors in quantitative analysis of soft, *Journal of Central South University (Natural Science Edition)*, 47(08), 2723-2729
- Song Yun-qi, Wu Chao-jun, Ye Guan-lin. 2018. Permeability and anisotropy of upper Shanghai clays. *Rock and Soil Mechanics* 39(06): 2139-2144.
- Tanaka H, Shiwakoti D R, Omukai N, et al. 2003. Pore size distribution of clayey soils measured by mecury instrusion porosimetry and its relation to hydraulic conductivity. *Journal of the Japanese Geotechnical Society* 43(6):63-73.
- Tavenas F, Leblond P, Jean P, et al. 1983. The permeability of natural soft clays. Part I: Methods of laboratory measurement. *Canadian Geotechnical Journal* 20(4):629-644.
- Wang Xiu-yan, Liu Chang-li. 2003. Discussion on seepage and release of water in deep clay. Chinese Journal of Geotechnical Engineering 25(3): 308-312.
- Witt K J, Brauns J. 1983. Permeability-anisotropy due to particle shape. *Journal of Geotechnical Engineering* 109(9):1181-1187.
- Xu Jie, Zhou Jian, Luo Ling-hui, et al. 2020. Study on anisotropic permeability model for mixed kaolin-montmorillonite clays. *Rock and Soil Mechanics* 41(2): 469-476.
- Yu Liang-gui, Zhou Jian, Wen Xiao-gui, et al. 2019. Factors influencing permeability anisotropy of remolded kaolin. *Journal of Zhejiang University (Engineering Science)* 53(02): 74-82.
- Zhou Jian, Deng Yi-liang, Cao Yang et al. 2014. Experimental study of microstructure of Hangzhou saturated clay during consolidation

- process. Journal of Central South University (Science and Technology) 45(6): 1998-2005.

 Zhou Jian, Xu Jie, Yu Liang-gui et al. 2019. Study on microscopic mechanism regarding permeability anisotropy of kaolin-montmorillonite mixed clays. Chinese Journal of Geotechnical Engineering 41(06): 1005-1013.